Desalination and Water Treatment
www.deswater.com
doi: 10.1080/19443994.2014.937763

56 (2015) 665–676
October

Taylor & Francis
Taylor & Francis Group

Textile dyebath wastewater decolorization by electrolytic processes: response surface optimization using IV-optimal design

Harpreet Singh[a,*], Garvit Singh[a], Manpreet S. Bhatti[b], Akepati S. Reddy[a]

[a]*School of Energy and Environment, Thapar University, Patiala, Punjab, India, Tel. +91 98769 07690; Fax: +91 175 2393548; email: Harryenv@gmail.com (H. Singh), Tel. +91 84393 79211; email: garv.choudhary@gmail.com (G. Singh), Tel. +91 95017 99899; email: siva19899@gmail.com (A.S. Reddy)*
[b]*Department of Botanical and Environmental sciences, Guru Nanak Dev University, Amritsar, Punjab, India, Tel. +91 94171 07598; email: mbhatti73@gmail.com*

Received 11 February 2014; Accepted 17 June 2014

ABSTRACT

The aim of the present study is to investigate the potential of electrolytic process on textile dyebath dump wastewater (sulfate concentration ~30 g/L) collected from the cotton fabric dyeing process to remove color and COD concentration. Four different electrode combinations were tested i.e. stainless steel–stainless steel, iron–iron, aluminum–aluminum, and iron (anode)–aluminum (cathode) for best removal efficiency and minimum power consumption along with sludge generation rate. The significant process parameters (voltage/current density and treatment time) were optimized for real industrial wastewater using response surface methodology approach. COD removal efficiency and color removal efficiency were taken as two responses. The best electrode combination was Fe–Al to achieve 75% COD removal efficiency and 91% color removal efficiency. The optimized process conditions are 7.6 V (1242 A/m^2) and 14 min treatment time consuming 59 kWh/kg of COD removal with sludge generation rate of 24.1 g/L.

Keywords: Electrocoagulation; Real dye wastewater; Response surface methodology (RSM); Optimization; Sulfate wastewater

1. Introduction

Textile processing industry is concerned with the dyeing, printing, and finishing of textiles (fibre/yarn/fabric/garment of cotton, polyester, acrylic, etc.). The processing is both water and energy intensive. Main steps involved in textile processing include; filling water, dosing dyes and chemicals, cooling and washing, draining out the liquid, and proceeding with the next step of processing. Requirements of cooling water to decrease the temperature of dyebath contents and saturated steam/ thermic fluid for heating to facilitate process reactions are thus also quite high.

Dyes, chemicals (sodium sulfate/sodium chloride, sodium hydroxide, sodium carbonate, sodium sulfite, sodium hydrosulfite, acetic acid, hydrogen peroxide, etc.), and other material inputs (leveling agents, wetting agents, anti-creasing agents, stabilizing agents, etc.) are also extensively used in the processing. Wastewater generated from the processing contains dissolved solids, many inorganic and organic dye residues (in cotton dyebath dump), and even

*Corresponding author.

suspended solids (mostly generated from the textile being processed).

Wastewaters generated at different process steps vary widely in their characteristics and strengths. Dye-bath dumps and dumps of chemical treatment steps are much stronger than the wastewaters generated from the rinsing/washing/cleaning steps.

Mixing of the wide varieties of wastewaters generated in a textile processing unit makes the decolorization of the effluent and its compliance, especially with the BOD/COD standards, difficult. Further, this mixing of the effluents results in reduced wastewater, recycle and reuse potential. Recovery of chemicals, residual inputs, products and by-products, and new resources is not viable because of the dilution occurring from the mixing. Further, the treated effluent may not be fit for reuse and water conservation may become difficult.

Various conventional techniques like biological, chemical, and physical methods have been used for the treatment of textile wastewater [1–6]. Fenton (H_2O_2 and Fe^{2+}), Fenton-like (H_2O_2 and Fe^{3+}), Photo-Fenton, Ozone, and UV/H_2O_2 are some of the advanced oxidation treatment methods, which were also applied to remove color [7,8]. The most commonly used chemical coagulation/precipitation–flocculation-settling induces secondary pollution from the added chemical substances (Alum, lime, and/or polymers) and generates large quantities of sludge with poor dewatering properties. This treatment process also tends to increase the total dissolved solids content of the wastewater.

Electroflocculation (EF) process has less reactive retention period; the treatment is done without adding any chemical coagulant or flocculant, thus reducing the amount of sludge [9]. The experiments suggest that electrolytically added aluminum ions are much more active than chemically added aluminum ions [10]. Flocs formed are similar to chemical floc, except that EF flocs are acid-resistant, more stable containing less-bound water and tend to be much larger in size, and therefore, can be separated faster by filtration. This process has the advantage of removing the smallest colloidal particles, because the applied electric field sets them in faster motion, thereby facilitating the coagulation.

EF is a combination of oxidation, coagulation, flocculation, and flotation [11]. Here, the flocculating agent is generated by electro-oxidation of a sacrificial anode, generally made of iron or aluminum. The electrochemical reactions occurring at the Al anode and cathode are-

$$\text{Anodic reaction} - \mathrm{Al(s)} \longrightarrow \mathrm{Al}^{3+} + 3e^- \tag{1a}$$

$$\text{Cathodic reaction} - 3\mathrm{H_2O} + 3\mathrm{e}^- \longrightarrow 3\mathrm{OH}^- + 3/2\mathrm{H_2} \tag{1b}$$

The electrochemical reactions occurring at the Fe anode and cathode are

$$\text{Anodic reaction} - \mathrm{Fe(s)} \longrightarrow \mathrm{Fe}^{2+} + 2\mathrm{e}^- \tag{2a}$$

$$\mathrm{Fe}^{2+} \longrightarrow \mathrm{Fe}^{3+} + \mathrm{e}^- \tag{2b}$$

$$\text{Cathodic reaction} - 2\mathrm{H_2O} + 2\mathrm{e}^- \longrightarrow 2\mathrm{OH}^- + \mathrm{H_2(g)} \tag{2c}$$

In this process, the coagulating ions are produced *in situ* and destabilize the colloidal pollutants, particulate suspension, and breaking of emulsions [12]. The destabilized particulates form flocs. Hydrolyzation of polymeric iron or aluminum hydroxides occurs immediately after the production of metal ions. Electrolytic gases, such as hydrogen are generated at the cathode which float some part of the flocs to the surface of the reactor.

Various studies have been reported on the potentials of electrocoagulation process [13] in the treatment of electroplating wastewater [14], phenol-formaldehyde resin manufacturing wastewater [15], Boron containing wastes [16], hexavalent-chromium containing water [17], dairy industry wastewater [18], distillery wastewater [19], melanoidins [20], nitrate-containing water [21], fluoride containing wastewater [22], metal-finishing effluents [23], groundwater containing arsenate [24], dyes wastewater [25–28], and synthetic textile wastewater [29]. Iron and aluminum [30], metal oxide-coated anodes [31], Ti/RuO_2, Ti/Pt, and Ti/Pt/Ir [32] electrodes are investigated for the treatment of textile wastewater.

Response Surface Methodology (RSM) is a collection of mathematical and statistical techniques, commonly used for developing, improving, and optimizing processes. It can be used to evaluate the relative significance of several affecting factors in the presence of complex interactions [33]. It uses an experimental design such as the composite central design to fit a model by least squares technique. The process efficiency in the EF process is generally affected by many factors. The optimization of these factors may significantly increase the process efficiency and maximize the pollutant removal. Recently, RSM has been successfully applied to optimize electrocoagulation process for the treatment of Reactive orange 107 [34], C.I. Acid Red 14 azo dye [35], Arsenic removal from drinking water [36], simulated beet sugar factory wastewater [37], textile dye wastewater [38] and to separate oil from oily wastewater emulsion [39].

In the present study, decolorization of the textile dyebath dump wastewater (sulfate rich), collected from the cotton fabric dyeing process, by electrolytic processes has been tried. Stainless steel, iron, aluminum, and iron-aluminum combination electrodes have been tried. The study was also focused on finding out the best sacrificial electrode material for the wastewater. Two process variables (voltage and treatment time) were varied as per IV-optimal design strategy of RSM. COD removal efficiency (Response I) and Color removal efficiency (Response II) were taken as responses. ANOVA model was constructed which best fits the response data. Energy consumptions and sludge formations were also studied separately.

2. Materials and methods

2.1. Materials

The wastewater used in the study was collected from a cotton textile processing industry located in Ludhiana, Punjab, India. The cotton textile dyeing process includes the use of Glauber's salt ($Na_2SO_4{\cdot}10H_2O$) as wetting agent to facilitate the dyeing action which also leads to maximum exhaustion of the dyes. Cotton textile dyebath dump wastewater was rich in sulfate and have the initial characteristics presented in Table 1.

2.2. Experimental set-up

The experimental setup used in the study is shown in Fig. 1. It included a reactor, a digital DC power system (0–30 V and 0–30 A), and a magnetic stirrer. The reactor was fabricated from 6 mm acrylic sheet and has 415 mL working volume. Its dimensions are 6.1 cm length, 4.7 cm width, and 33.3 cm height. Two electrodes each of 4.9 cm width, 20 cm length, and 3 mm thickness were used as the anode and the cathode inside the reactor. Effective electrode area of the electrode was 98 cm^2. Four different pairs of electrodes, namely, Al–Al, Fe–Fe, SS–SS, and Fe–Al were used in the present study. With the help of grooves in the reactor wall, gap between the two electrodes was maintained at 10 mm. For mixing, a 2.3 cm long magnetic bit was used and the reactor was placed over a magnetic stirrer. A DC power supply system (ELNOVA Ltd, New Delhi – Model No. 664300300D with input 230 V/AC) was used. This system was capable of supplying DC power in the range of 0–30 V and 0–30 A. The system had a provision to regulate voltage and DC current supply. Further, the system had provisions for metering the power (both voltage and amperage) being supplied to the reactor.

2.3. Design of experiments and approach followed

EF treatment of cotton textile dyebath dump sulfate-rich wastewater was studied using the following four electrode combinations:

(1) Al–Al
(2) Fe–Fe
(3) SS–SS
(4) Fe–Al

The parameters and the responses were selected initially from the published literature and from the understanding of the EF process. Through preliminary studies the parameters for the final study and their ranges were selected. Voltage and time were used as parameters and Color, COD, power consumption, and sludge generation were used as responses. A set of 19 experiments were finalized, through design of experiments, for the EF treatment on sulfate-rich wastewater and for all the four combinations of electrodes.

IV-optimal design strategy of RSM with Design Expert Software was used for the design of experiments. Total 19 experiments were included; six model points, five replicates at center point, and additional three center runs and five runs for estimating the *Lack of fit*. The 19 experiments are presented in Table 2.

Filtered wastewater was taken into the reactor, the electrodes were positioned in the reactor, voltage was adjusted to the desired value, and the current was passed through for the set duration. Amperage was monitored at regular intervals (30 s or 1 min intervals). The Polarity of the electrodes was interchanged intermittently to improve the performance of EF. Magnetic stirring was applied in the reactor while performing EF to treat homogenous samples. After treatment, the treated wastewater was filtered and the filtered sample was analyzed for COD, Color, Conductivity, and pH. Sludge generated was measured gravimetrically. Current density and power consumptions were also estimated. The surface of electrode plates was rinsed with water after every experimental run, to inhibit the electrode passivation process. The removal efficiencies of COD and Color were calculated. The results obtained were compiled. The APHA methods [40] have been followed for analytical techniques used in the characterization of wastewater and for monitoring the responses.

Table 1
Characteristics of initial and optimum conditions (Fe–Al) of cotton textile dyebath dump wastewater

S. no.	Parameter (units)	Initial value	Values – optimum conditions (Fe–Al)	Techniques	Instruments
1	Color (Pt Co units)	1,000	85	Direct spectrophoto meter at 455 nm	HACH DR/2000 Direct Spectrophotometer
2	COD (mg/L)	1,243	304.5	Open reflux titrimetric	Spectralab COD Digestor 2015 M
3	Turbidity (NTU)	217	–	Nephelometric	Elico CL 52D Nephelometer
4	Conductivity (mS/cm)	51.2	–	Electrometric	Thermo Orion model 555 A
5	pH	10.8	11.6	Electrometric	Li 127, pH meter- Elico pvt. Ltd.
6	TDS (mg/L)	61,203	60,895	Gravimetric	Analytical balance (AG135 Mettler Toledo)
7	TSS (mg/L)	27	–	Gravimetric	Analytical balance (AG135 Mettler Toledo)
8	Sulphate (mg/L)	29,134	29,080	Gravimetric with ignition of residue	Muffle furnace (Abrostate E/101/D)
9	Total Alkalinity (mg/L as $CaCO_3$)	13,053	9,763	Titrimetric	–
10	Sodium (mg/L)	19,400	19,286	Flame emission photometric	Flame Photometer ESICO model 1,382
11	Chloride (mg/L)	645	623	Argentometric	–
12	Surfactants (ppm)	<0.1	<0.1	Anionic surfactants as MBAS	UV–vis spectrophotometer Analytik jena specord 200
13	Phenols (ppm)	<0.1	<0.1	Direct photometric	UV–vis spectro photometer Analytik jena specord 200
14	Sulfide (mg/L)	10.4	3.2	Iodometric	–
15	Sulfite (mg/L)	5	1	Iodometric	–
16	Calcium (mg/L)	41.3	2.5	Direct air-acetylene flame method	Atomic absorption spectrophotometer GBC 932 AA
17	Magnesium (mg/L)	20.4	<0.01	Direct air-acetylene flame method	Atomic absorption spectrophotometer GBC 932 AA

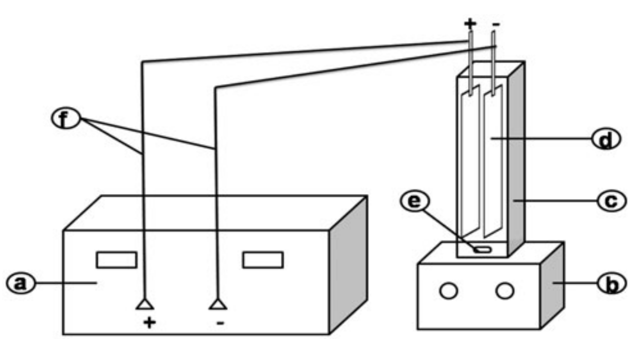

Fig. 1. Schematic diagram of experimental set-up (a) DC power supply (b) magnetic stirrer (c) reactor (d) electrode (e) magnetic bit (f) interconnecting wires.

3. Results and discussion

Results obtained from the laboratory experimentation with different electrodes are presented in Table 3. With Al–Al electrodes, the maximum removal efficiencies for COD and Color came out to be 61 and 81.6%, respectively, at 12 V and 15 min treatment time. A sludge generation rate of 13.6 g/L was obtained. A current density of 785.7 A/m^2 and a power consumption of 62.4 kWh/m^3 were also observed. Above pH 10, soluble species of $Al(OH)_4^-$ is the predominant hydrolysis product which tends to drop the COD removal efficiency and this is in accordance with the amphoteric character of aluminum hydroxide $Al(OH)_3$ that precipitates at pH 6–7. The initial pH of wastewater was a key parameter with Al–Al electrodes. The removal efficiency of COD was 61.1% at 785.7 A/m^2, 39.7% at 606.6 A/m^2, and 31.5% at 284.2 A/m^2, after 12 V treatments with Al–Al electrodes. At high-current density, the extent of anodic dissolution of aluminum increases resulting in greater amount of precipitate and COD removal [41].

The maximum removal efficiencies of 73.9 and 95.7% for COD and Color, respectively, were observed when treated with Fe–Fe electrodes at 12 V for 15 min treatment time. 24.6 g/L of sludge was generated at current density of 3193.8 A/m^2 and power consumption of

Table 2
Set of Experimental design as per IV optimal design

S. no.	Factor 1: voltage (V)	Factor 2: treatment time (min)
1	12	15
2	4	15
3	12	15
4	4	15
5	4	3
6	12	3
7	12	3
8	10	6
9	6.6	12.9
10	5.8	5.7
11	9.6	12.6
12	8	9
13	8	9
14	8	9
15	12	9.6
16	7.6	3
17	4	8.4
18	4	8.4
19	7.6	3

240.7 kWh/m^3. An increase in current density increases the amount of sludge and also increases power consumption. Sludge generation with Fe–Fe electrodes is more than Al–Al electrodes as Fe is heavier than Al and it induces the formation of higher floc sizes [42]. The COD and Color removal efficiency is higher in Fe–Fe electrodes than Al–Al electrodes. This agrees with the literature on Orange II, mono-azo acid dye [43].

The SS–SS electrodes were not efficient as it gives only 42% and 9% maximum removal efficiency for COD and Color at 12 V 15 min and 4 V 8.4 min, respectively. Sludge generation rate is observed least for SS electrodes irrespective of the higher current density. Electrolytic process using SS electrodes appeared to be less efficient than other electrode combinations in present study. Therefore, it is observed that COD and Color removal efficiency with SS were much lower than those obtained from experiments with other electrode combinations. The Fe–Al electrodes gave 73.8 and 95% maximum removal efficiency for COD and Color, respectively, at 10 V and 6 min treatment time. The sludge generation rate of 25.8 g/L was observed for this experimental run at current density of 2,381 A/m^2 and power consumption of 61.4 kWh/m^3.

In Fe–Al electrode treatment, for the increase in current density from 51 to 2,937 A/m^2, the decolorization rate increases from 3 to 93.5%. Applying current density of 2,381 A/m^2 leads to a decolorization rate of 95%. This agrees with the literature in which by doubling the current density from 5.46 to 10.91 A/m^2, the decolorization rate increases from 49.2 to 98.9% for the removal of indigo carmine dye [44]. In present study, no significant changes were observed with respect to pH and conductivity (σ), after treatment with all four electrode combinations, with respect to original σ of 51.2 and pH of 10.8 units.

From the obtained results, only Fe–Al electrodes showed promising results, thus it is used for statistical modeling for given textile sulfate-rich wastewater. Response surface methodology was used for the process optimization. While treating with SS–SS electrode, the maximum removal efficiency for COD is 42% only and 17 out of 19 values came out to be negative for color removal, thus it was impossible to fit the model. The model with Al–Al electrode had low prediction capability. The model with Fe–Fe treatment had serious problem with *Lack of fit*, which indicates that the model signal is low as compared to noise. The maximum removal efficiency for responses was achieved with Fe–Al electrodes and here also the model navigates in design space. With the help of Design Expert Software (trial version 8.0), ANOVA model was constructed which best fits the response data. For checking experimental reproducibility, which is the major issue in RSM, the sequential experimental designs were performed, whose values were obtained from the best solutions from the Design expert software. The experimental design as per IV-optimal criteria

Table 3
Results of experimentation on sulphate rich wastewater with different electrodes

Electrodes	Voltage (V)	Time (min)	Current density (A/m^2)	Color (Pt Co Units)	COD (mg/L)	Conductivity (mS/cm)	pH	Power consumption (kWh/m^3)	Sludge generation rate (g/L)
Al–Al	12	15	653	227	549	51.5	11.1	51.9	14.4
Al–Al	4	15	492	364	575	50.5	11.2	13.0	13.3
Al–Al	12	15	785	184	484	50.8	11.4	62.4	13.6
Al–Al	4	15	429	870	609	51.8	10.6	11.3	12.9
Al–Al	4	3	144	1,200	924	52.6	10.1	0.7	9.4
Al–Al	12	3	284	1,120	851	50.8	10.3	4.5	10.4
Al–Al	12	3	301	720	786	50.7	10.4	4.8	10.4
Al–Al	10	6	188	930	931	50.7	10.2	4.9	7.9
Al–Al	6.6	12.9	344	880	857	51.9	10.1	12.9	7.6
Al–Al	5.8	5.7	207	970	948	50.6	10.6	3.0	7.5
Al–Al	9.6	12.6	433	550	783	51.6	10.2	23.1	8.5
Al–Al	8	9	486	566	743	50.2	10.3	15.4	8.3
Al–Al	8	9	427	730	873	51.9	10.2	13.5	9.4
Al–Al	8	9	406	750	865	51.8	10.1	12.9	9.7
Al–Al	12	9.6	606	640	750	51.6	10.2	30.8	10.6
Al–Al	7.6	3	332	970	989	51.2	10.6	3.3	7.6
Al–Al	4	8.4	456	760	923	50.5	10.0	6.7	7.4
Al–Al	4	8.4	482	880	956	51.5	10.3	7.1	6.0
Al–Al	7.6	3	357	740	914	50.2	9.7	3.5	7.9
Fe–Al	12	15	2,152	90	449	54.6	11.6	166.4	50.5
Fe–Al	4	15	326	507	606	52.4	10.8	8.4	10.3
Fe–Al	12	15	2,358	100	412	54.3	11.2	182.4	50.0
Fe–Al	4	15	285	680	864	53.3	11.0	7.3	9.8
Fe–Al	4	3	51	970	1,220	53.4	10.7	0.3	3.2
Fe–Al	12	3	2,479	73	379	51.2	10.9	38.4	17.4
Fe–Al	12	3	2,937	65	362	51.8	11.1	45.4	18.1
Fe–Al	10	6	2,381	50	326	53.2	11.8	61.4	25.8
Fe–Al	6.6	12.9	1,062	33	339	52.9	11.8	38.9	22.1
Fe–Al	5.8	5.7	363	500	714	52.5	10.2	5.15	8.9
Fe–Al	9.6	12.6	1,809	60	367	54.8	10.9	94.0	32.9
Fe–Al	8	9	1,336	36	343	53.7	10.9	41.3	23.6
Fe–Al	8	9	1,390	33	360	53.4	10.8	43.0	21.7
Fe–Al	8	9	1,450	30	387	53.9	11.4	44.9	21.1
Fe–Al	12	9.6	2,395	104	444	52.3	10.8	118.6	42.0
Fe–Al	7.6	3	733	522	680	53.2	10.3	7.1	7.1
Fe–Al	4	8.4	162	900	1,200	53.4	10.9	2.3	9.1
Fe–Al	4	8.4	241	553	920	52.7	10.6	3.4	8.4
Fe–Al	7.6	3	627	465	680	53.7	10.7	6.1	6.3
Fe–Fe	12	15	3,193	43	324	54.7	10.9	240.7	24.6
Fe–Fe	4	15	456	23	562	53.2	11.9	11.4	8.2
Fe–Fe	12	15	3,119	50	335	54.9	10.5	235.1	28.2
Fe–Fe	4	15	525	27	554	51.9	10.0	13.2	8.1
Fe–Fe	4	3	483	497	752	51.8	9.2	2.4	3.7
Fe–Fe	12	3	3,058	90	407	51.8	9.2	46.1	11.2
Fe–Fe	12	3	3,109	80	403	50.8	10.7	46.8	10.5
Fe–Fe	10	6	2,756	23	353	52.0	10.8	69.2	12.7
Fe–Fe	6.6	12.9	1,371	25	404	52.6	11.2	48.9	11.7
Fe–Fe	5.8	5.7	1,034	43	746	51.9	11.4	14.3	6.5
Fe–Fe	9.6	12.6	2,985	23	506	52.7	11.8	151.2	20.8
Fe–Fe	8	9	1,833	36	590	51.7	11.7	55.2	15.0

(*Continued*)

Table 3 (*Continued*)

Electrodes	Voltage (V)	Time (min)	Current density (A/m^2)	Color (Pt Co Units)	COD (mg/L)	Conductivity (mS/cm)	pH	Power consumption (kWh/m^3)	Sludge generation rate (g/L)
Fe–Fe	8	9	1,578	25	618	51.7	11.3	47.6	14.6
Fe–Fe	8	9	772	43	612	51.7	11.2	53.4	15.1
Fe–Fe	12	9.6	3,180	23	561	52.2	11.5	153.4	24.0
Fe–Fe	7.6	3	1,218	149	652	50.9	11.8	11.6	8.1
Fe–Fe	4	8.4	383	66	659	52.2	11.3	5.3	8.9
Fe–Fe	4	8.4	373	100	713	52.3	11.7	5.2	9.0
Fe–Fe	7.6	3	1,460	146	576	50.7	11.6	13.9	8.0
SS–SS	12	15	2,834	2,120	796	53.8	10.5	231.5	6.2
SS–SS	4	15	369	1,170	894	50.7	10.6	10.0	3.6
SS–SS	12	15	2,914	2,210	718	54.5	10.5	238.0	6.0
SS–SS	4	15	397	1,030	906	51.0	10.7	10.8	3.1
SS–SS	4	3	278	1,070	918	51.5	10.6	1.5	3.1
SS–SS	12	3	2,931	1,560	808	52.7	10.6	47.8	5.0
SS–SS	12	3	3,173	1,560	828	51.8	10.6	51.8	5.4
SS–SS	10	6	2,595	1,600	800	52.1	10.6	70.6	4.6
SS–SS	6.6	12.9	1,245	1,410	783	51.5	10.6	48.1	4.4
SS–SS	5.8	5.7	919	1,300	972	51.1	10.6	13.7	4.4
SS–SS	9.6	12.6	2,696	1,580	799	51.8	10.1	148.0	7.1
SS–SS	8	9	1,528	1,400	873	51.0	10.7	49.9	7.0
SS–SS	8	9	1,586	1,390	849	52.3	10.6	51.8	6.3
SS–SS	8	9	1,510	1,500	865	51.5	10.5	49.3	8.0
SS–SS	12	9.6	3,043	1,560	824	50.6	10.4	159.0	6.9
SS–SS	7.6	3	1,010	1,050	1,030	50.1	10.5	10.4	6.0
SS–SS	4	8.4	216	990	1,071	50.6	10.7	3.3	3.3
SS–SS	4	8.4	193	910	939	50.2	10.6	2.9	3.8
SS–SS	7.6	3	1,247	1,210	1013.5	51.0	10.4	12.9	7.2

with actual and predicted removal efficiencies for Fe–Al electrode combinations are presented in Table 4 and the ranges of different responses for different combination of electrodes are presented in Table 5.

3.1. Statistical modeling for COD and Color removal efficiency with Fe–Al electrodes

3.1.1. Statistical modeling for COD removal efficiency

The ANOVA sequential model sum of squares proposed quadratic model as best fit models. Backward elimination method was applied to remove any non significant model terms. This eliminates the square term for treatment time. Reduced ANOVA model was again generated and the fitted quadratic model has 99.99% significance level ($F = 38.5$, degree of freedom $= 4$) with *Lack of fit* not significant (p-value $= 0.693$). The results of ANOVA statistics for COD removal are given in Table 6. The CV of 14.24% and predicted $R^2 = 0.834$ was close to adjusted R^2 of 0.893. Also, S/N ratio of 20.6 indicated that model noise is not significant as compared to signal. Thus, model could be navigated in the design space. The unit-less regression equation in terms of coded factors is given in Eq. (1) and in terms of actual factors in Eq. (2).

$$\text{COD removal eff.}(\%) = +67.61 + 23.66 \times \text{A} + 10.81 \times \text{B} - 12.23\text{A} \times \text{B} - 24.43 \times \text{A}^2 \tag{1}$$

where A: Voltage and B: Treatment time is in coded units.

$$\text{COD removal eff.}(\%) = -130.328 + 34.930\ \text{V} + 5.877 \times \text{min} - 0.50943\ \text{V} \times \text{min} - 1.52686\ \text{V}^2 \tag{2}$$

Table 4
Experimental design as per IV-optimal criteria with actual and predicted removal efficiencies for Fe–Al electrode combinations

S. no.	Factor 1 A: voltage (V)	Factor 2 B: treatment time (min)	Response 1 COD removal eff. (%) Actual	Response 1 COD removal eff. (%) Predicted	Response 2 Color removal eff. (%) Actual	Response 2 Color removal eff. (%) Predicted
1	5.84	5.75	42.56	38.27	50.00	51.27
2	12.00	9.60	64.28	66.70	89.60	101.49
3	10.00	6.00	73.77	70.98	95.00	96.05
4	7.61	3.00	45.29	53.07	47.80	60.43
5	8.00	9.00	72.41	67.61	96.40	91.80
6	8.00	9.00	68.87	67.61	97.00	91.80
7	4.00	8.40	25.99	17.21	44.70	29.82
8	9.60	12.60	70.47	76.72	94.00	101.65
9	8.00	9.00	71.12	67.61	96.70	91.80
10	4.00	8.40	3.46	17.21	10.00	29.82
11	12.00	15.00	66.85	65.43	90.00	88.73
12	4.00	15.00	51.25	42.56	49.30	44.38
13	12.00	15.00	63.88	65.43	91.00	88.73
14	7.61	3.00	45.29	53.07	53.50	60.43
15	12.00	3.00	69.51	68.26	92.70	87.33
16	4.00	3.00	1.85	−3.52	3.00	−6.42
17	6.58	12.87	72.73	65.91	96.70	82.07
18	12.00	3.00	70.88	68.26	93.50	87.33
19	4.00	15.00	30.49	42.56	32.00	44.38

Table 5
Ranges of different responses for different electrode combinations

Electrode combinations	Fe–Fe	Fe–Al (optimum)	Al–Al	SS–SS
COD removal (%)	39.5–73.9	1.8–73.8 (75.5)	20.4–61.1	13.8–42.2
Color removal (%)	50.3–97.7	3.0–97.0 (91.5)	Maximum 81.6	Maximum 9.0
Current density (A/m^2)	373.5–3193.9	51.0–2937.0 (1,242)	144.3–785.7	193.9–3043.9
Power consumption (kWh/m^3)	2.4–240.8	0.3–182.4 (55.3)	0.8–62.4	1.5–238.0
Sludge generation rate (g/L)	3.7–28.2	3.2–50.5 (24.1)	6.0–14.4	3.1–8.0

Values given in parenthesis is at optimized conditions.

where A: Voltage (V) and B: Treatment time (min) are in actual units.

Before moving to the response surface plots, diagnostic statistics were studied using normal plot of residuals to satisfy the normal distribution of error as given in Fig. 2(a). The actual vs. predicted response plot for percentage swelling is given in Fig. 2(b). The response plots were generated using regression equations. COD removal efficiency was taken as response, and voltage and treatment time varied in the designed space. The maximum COD removal efficiency of 75% was obtained at 7.6 V and 14 min treatment time. Whereas, just 2% COD removal efficiency was obtained at 4 V and 3 min. The 3D contour plot between COD removal efficiency vs. voltage and treatment time is given in Fig. 3. There is antagonistic interaction between voltage and treatment time and this indirectly indicated that one of them should be minimized and another should be maximized. Looking at unit-less regression coefficients in Eq. (1), it is advisable to maximize treatment time and minimize the voltage to get best results.

3.1.2. Statistical modeling for color removal efficiency

Similarly Color removal efficiency was modeled and best fitted equations for unit-less and actual are given in Eqs. (3) and (4), respectively.

Table 6
Results of ANOVA statistics for COD removal for Fe–Al electrode combinations

Source	Sum of squares	df	Mean squares	F-value	p-value Prob > F
Model	8,845	4	2,211	38.5	<0.0001*
A-voltage (V)	6,004	1	6,004	105	<0.0001*
B-treatment time (min)	1,140	1	1,140	20	0.0005*
A × B	1,064	1	1,064	19	0.0007*
A^2	2,267	1	2,267	39	<0.000*
Lack of fit	323	7	46	1	0.6934#
*Significant at $p < 0.05$					
#Not significant at $p < 0.05$					
Std. dev.	7.579		R^2	0.917	
Mean	53.207		Adjusted R^2	0.893	
C.V. %	14.244		Predicted R^2	0.834	

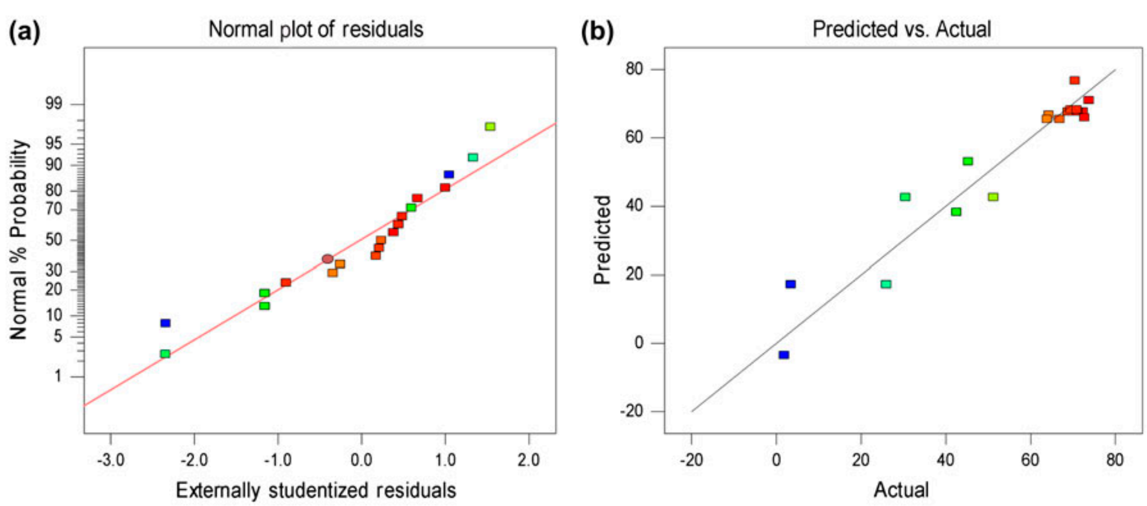

Fig. 2. (a) Normal probability plot and (b) Actual vs. Predicted plot for COD removal efficiency for Fe–Al electrode combinations.

$$\text{Color rem. eff.} (\%) = +91.80 + 34.53\ A + 13.05\ B - 12.35 A \times B - 24.78\ A^2 - 13.52\ B^2 \quad (3)$$

where A: Voltage and B: Treatment time is in coded units.

$$\text{Color rem. eff.} (\%) = -163.412 + 38.041\ V + 13.052\ \text{min} - 0.514\ V \times \text{min} - 1.548\ V^2 - 0.375\ \text{min}^2 \quad (4)$$

where A: Voltage (V) and B: Treatment time (min) are in actual units.

The results of ANOVA statistics for color removal are presented in Table 7. Numerical optimization was achieved through desirability plot by simultaneously solving fitted models. The 3D contour plot between color removal efficiency vs. voltage and treatment time is given in Fig. 4. The independent variables were set within the range and COD removal efficiency was set as maximimum and color removal efficiency was set within the range. Through random sampling point, best process conditions were achieved at 7.6 V and 14 min to achieve 75% COD removal efficiency and 91% color removal efficiency. The results were verified by validation testing at new proposed conditions. The COD and color comes out to be 304.5 mg/L and 85 Pt. Co. unit, respectively, which ensures the

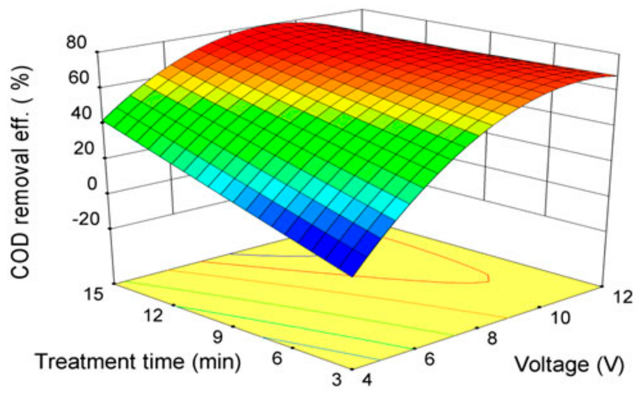

Fig. 3. Three dimensional contour plot showing COD removal efficiency vs. voltage and treatment time for Fe–Al electrode combinations.

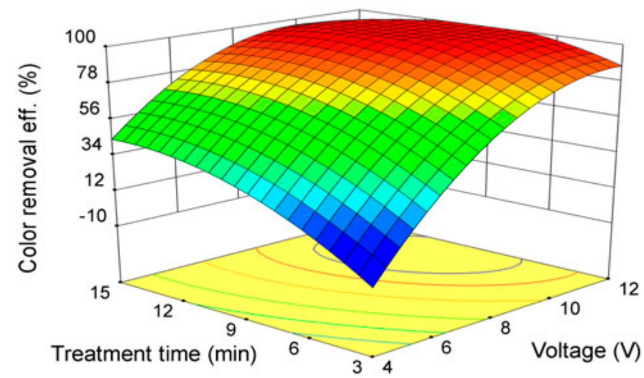

Fig. 4. Three dimensional contour plot showing Color removal efficiency vs. voltage and treatment time for Fe–Al electrode combinations.

Table 7
Results of ANOVA statistics for Color removal for Fe–Al electrode combinations

Source	Sum of squares	df	Mean squares	*F*-value	*p*-value Prob > *F*
Model	16,459	5	3,292	26	<0.0001*
A-voltage (V)	12,531	1	12,531	99	<0.0001*
B-treatment time (min)	1,639	1	1,639	13	0.0033*
AxB	1,078	1	1,078	8	0.0121*
A^2	2,013	1	2,013	16	0.0016*
B^2	582	1	582	5	0.0517*
Lack of fit	881	6	147	1	0.3532#
*Significant at $p < 0.05$					
#Not significant at $p < 0.05$					
Std. dev.	11.267		R^2	0.909	
Mean	69.626		Adjusted R^2	0.874	
C.V. %	16.182		Predicted R^2	0.782	

reliability of response functions predictions as presented as values at optimum conditions in Table 1. The current density and power consumption are 1,242 A/m^2 and 55.3 kWh/m^3, respectively, with sludge generation rate of 24.15 g/L. The 2.54 mg/L calcium is detected i.e. 94% is removed, whereas there is no variations obtained for total dissolved solids, sulfate, chloride, Na, and Mg in treated wastewater at optimum conditions. The wastewater after treatment can be concentrated for salt recovery.

4. Conclusions

In this study, electrolytic treatment of sulfate-rich textile dyebath dump wastewater was tried using four electrode combinations viz. Fe–Fe, Fe (Anode)–Al (Cathode), Al–Al, and SS–SS. Response surface methodology fitted well the experimental data for Fe–Al electrode combination and gave 75 and 91% COD and color removal efficiencies, respectively, with 55.3 kWh/m^3 of power consumption. Antagonistic Interaction between voltage and treatment time was observed, which indicated low voltage and higher treatment time for best results. Although, experimental data for other electrode combinations could not be fitted well using regression modeling. Under best operating conditions, Fe–Fe electrode combination gave 74% and 97% removal efficiency for COD and color, respectively. Al–Al electrode combination gave maximum COD removal of 61% and the power consumption is lowest among all the four combinations, which suggests Al–Al combination as pretreatment method. SS–SS electrode combination was found ineffective in decolorizing the textile wastewater with 42% COD removal (max.) under best operating conditions. The dyebath dump wastewater can easily be reused after the decolorization treatment and treated water can be used as process water to reduce the consumption of glauber's salt and hence sodium sulfate in the dyebath preparation.

References

[1] J. Mo, J. Hwang, J. Jegal, J. Kim, Pretreatment of a dyeing wastewater using chemical coagulants, Dyes Pigm. 72(2) (2007) 240–245.

[2] A.H. Hassani, S. Seif, A.H. Javid, M. Borghei, Comparison of adsorption process by GAC with novel formulation of coagulation-flocculation for color removal of textile wastewater, Int. J. Environ. Res. 2(3) (2008) 239–248.

[3] B.Y. Gao, Q.Y. Yue, Y. Wang, W.Z. Zhou, Color removal from dye-containing wastewater by magnesium chloride, J. Environ. Manage. 82(2) (2007) 167–172.

[4] M.T. Sulak, H.C. Yatmaz, Removal of textile dyes from aqueous solutions with eco-friendly biosorbent, Desalin. Water Treat. 37(1–3) (2012) 169–177.

[5] S.L. Lim, W.L. Chu, S.M. Phang, Use of Chlorella vulgaris for bioremediation of textile wastewater, Bioresour. Technol. 101(19) (2010) 7314–7322.

[6] I. Petrinić, N.P.R. Andersen, S. Šostar-Turk, A.M. Le Marechal, The removal of reactive dye printing compounds using nanofiltration, Dyes Pigm. 74(3) (2007) 512–518.

[7] S.A. Abo-Farha, Comparative study of oxidation of some azo dyes by different advanced oxidation processes: Fenton, fenton-like, photo-fenton and photo-fenton-like, J. Am. Sci. 6(10) (2010) 128–142.

[8] H. Amin, A. Amer, A.E. Fecky, I. Ibrahim, Treatment of textile wastewater using H_2O_2/UV system, Physicochem. Probl. Mi. 42 (2008) 17–28.

[9] E. Yuksel, M. Eyvaz, E. Gurbulak, Electrochemical treatment of colour index reactive orange 84 and textile wastewater by using stainless steel and iron electrodes, Environ. Prog. Sust. Energy 32(1) (2013) 60–68.

[10] J.C. Donini, J. Kan, J. Szynkarczuk, T.A. Hassan, K.L. Kar, The operating cost of electrocoagulation, Can. J. Chem. Eng. 72(6) (1994) 1007–1012.

[11] J.P.F. Koren, U. Syversen, State-of-the-art electroflocculation, Filtr. Sep. 32(2) (1995) 153–156, 146.

[12] C. Barrera-Díaz, B. Bilyeu, G. Roa, L. Bernal-Martinez, Physicochemical Aspects of Electrocoagulation, Sep. Purif. Rev. 40(1) (2011) 1–24.

[13] O. Sahu, B. Mazumdar, P.K. Chaudhari, Treatment of wastewater by electrocoagulation: A review, Environ. Sci. Pollut. Res. 21(4) (2014) 2397–2413.

[14] N. Adhoum, L. Monser, N. Bellakhal, J. Belgaied, Treatment of electroplating wastewater containing Cu^{2+}, Zn^{2+} and Cr(VI) by electrocoagulation, J. Hazard. Mater. 112 (3) (2004) 207–213.

[15] M. Ahmadi, H. Amiri, S.S. Martínez, Treatment of phenol-formaldehyde resin manufacturing wastewater by the electrocoagulation process, Desalin. Water Treat. 39(1–3) (2012) 176–181.

[16] Y. Xu, Electrocoagulation: A new approach for the removal of boron containing wastes, Desalin. Water Treat. 2(1–3) (2009) 133–140.

[17] M.S. Bhatti, A.S. Reddy, R.K. Kalia, A.K. Thukral, Modeling and optimization of voltage and treatment time for electrocoagulation removal of hexavalent chromium, Desalination 269 (2011) 157–162.

[18] G.F.S. Valente, R.C. Santos Mendonça, J.A.M. Pereira, L.B. Felix, The efficiency of electrocoagulation in treating wastewater from a dairy industry, Part I: Iron electrodes, J. Environ. Sci. Health B 47(4) (2012) 355–361.

[19] Y. Yavuz, EC and EF processes for the treatment of alcohol distillery wastewater, Sep. Purif. Technol. 53(1) (2007) 135–140.

[20] M. Kobya, E. Gengec, Decolourization of melanoidins by a electrocoagulation process using aluminium electrodes, Environ. Technol. 33(21) (2012) 2429–2438.

[21] J. Lakshmi, G. Sozhan, S. Vasudevan, Recovery of hydrogen and removal of nitrate from water by electrocoagulation process, Environ. Sci. Pollut. Res. 20 (2013) 2184–2192.

[22] F. Shen, X. Chen, P. Gao, G. Chen, Electrochemical removal of fluoride ions from industrial wastewater, Chem. Eng. Sci. 58(3–6) (2003) 987–993.

[23] A. Khelifa, S. Moulay, A.W. Naceur, Treatment of metal finishing effluents by the electroflotation technique, Desalination 181(1–3) (2005) 27–33.

[24] I. Ali, T.A. Khan, M. Asim, Removal of arsenate from groundwater by electrocoagulation method, Environ. Sci. Pollut. Res. 19 (2012) 1668–1676.

[25] T.H. Kim, C. Park, E.B. Shin, S. Kim, Decolorization of disperse and reactive dyes by continuous electrocoagulation process, Desalination 150(2) (2002) 165–175.

[26] R. Bhatnagar, H. Joshi, I.D. Mall, V.C. Srivastava, Electrochemical treatment of acrylic dye-bearing textile wastewater: Optimization of operating parameters, Desalin. Water Treat. 52(1–3) (2014) 111–122.

[27] N.M. Mahmoodi, A. Dalvand, Treatment of colored textile wastewater containing acid dye using electrocoagulation process, Desalin. Water Treat. 51(31–33) (2013) 5959–5964.

[28] İ. Ayhan Şengil, A. Özdemir, Simultaneous decolorization of binary mixture of blue disperse and yellow basic dyes by electrocoagulation, Desalin. Water Treat. 46(1–3) (2012) 215–226.

[29] B. Merzouk, B. Gourich, A. Sekki, K. Madani, Ch. Vial, M. Barkaoui, Studies on the decolorization of textile dye wastewater by continuous electrocoagulation process, Chem. Eng. J. 149(1–3) (2009) 207–214.

[30] M. Kobya, O.T. Can, M. Bayramoglu, Treatment of textile wastewaters by electrocoagulation using iron and aluminium electrodes, J. Hazard. Mater. 100(1–3) (2003) 163–178.

[31] A.N.S. Rao, V.T. Venkatarangaiah, Metal oxide-coated anodes in wastewater treatment, Environ. Sci. Pollut. Res. 21(5) (2014) 3197–3217.

[32] J. Naumczyk, L. Szpyrkowicz, F. Zilio-Grandi, Electrochemical treatment of textile wastewater, Water Sci. Technol. 34(11) (1996) 17–24.

[33] R.H. Myers, D.C. Montgomery, C.M. Anderson-cook, Response surface methodology: Process and product optimization using designed experiments, third ed., Wiley, Hoboken, NJ, 2009.

[34] K. Rajkumar, M. Muthukumar, Optimization of electro-oxidation process for the treatment of reactive orange 107 using response surface methodology, Environ. Sci. Pollut. Res. 19 (2012) 148–160.

[35] A. Aleboyeh, N. Daneshvar, M.B. Kasiri, Optimization of C.I. Acid Red 14 azo dye removal by electrocoagulation batch process with response surface methodology, Chem. Eng. Process. 47(5) (2008) 827–832.
[36] M. Kobya, E. Demirbas, U. Gebologlu, M.S. Oncel, Y. Yildirim, Optimization of arsenic removal from drinking water by electrocoagulation batch process using response surface methodology, Desalin. Water Treat. 51(34–36) (2013) 6676–6687.
[37] G. Güven, A. Perendeci, A. Tanyolaç, Electrochemical treatment of simulated beet sugar factory wastewater, Chem. Eng. J. 151(1–3) (2009) 149–159.
[38] B.K. Körbahti, Response surface optimization of electrochemical treatment of textile dye wastewater, J. Hazard. Mater. 145(1–2) (2007) 277–286.
[39] M. Tir, N. Moulai-Mostefa, Optimization of oil removal from oily wastewater by electrocoagulation using response surface method, J. Hazard. Mater. 158(1) (2008) 107–115.
[40] APHA, AWWA, WEF, Standard methods for the examination of water and wastewater, 22nd ed., American Public Health Association, American Water Works Association and Water Environment Federation, Washington, DC, 2012.
[41] U.T. Un, A.S. Koparal, U.B. Ogutveren, Electrocoagulation of vegetable oil refinery wastewater using aluminium electrodes, J. Environ. Manage. 90(1) (2009) 428–433.
[42] S. Kara, E. Gurbulak, M. Eyvaz, E. Yuksel, Treatment of winery wastewater by electrocoagulation process, Desalin. Water Treat. 51(28–30) (2013) 1–9.
[43] M. Chafi, B. Gourich, A.H. Essadki, C. Vial, A. Fabregat, Comparison of electrocoagulation using iron and aluminium electrodes with chemical coagulation for the removal of a highly soluble acid dye, Desalination 281 (2011) 285–292.
[44] M.S. Secula, I. Creţescu, S. Petrescu, An experimental study of indigo carmine removal from aqueous solution by electrocoagulation, Desalination 277(1–3) (2011) 227–235.